Curvature corrections remove the inconsistencies of binary classical nucleation theory

Ailo Aasen,[1,2] David Reguera,[3,4] and Øivind Wilhelmsen[1,2]

[1] *Department of Energy and Process Engineering, Norwegian University of Science and Technology, NO-7491 Trondheim, Norway*
[2] *SINTEF Energy Research, NO-7465 Trondheim, Norway**
[3] *Departament de Física de la Matèria Condensada, Universitat de Barcelona, Martí i Franquès 1, 08028-Barcelona, Spain*
[4] *University of Barcelona Institute of Complex Systems (UBICS), Martí i Franquès 1, 08028 Barcelona, Spain*

(Dated: January 30, 2020)

The study of nucleation in fluid mixtures exposes challenges beyond those of pure systems. A striking example is homogeneous condensation in highly surface-active water–alcohol mixtures, where classical nucleation theory yields an unphysical, negative number of water molecules in the critical embryo. This flaw has rendered multicomponent nucleation theory useless for many industrial and scientific applications. Here, we show that this inconsistency is removed by properly incorporating the curvature dependence of the surface tension of the mixture into classical nucleation theory for multicomponent systems. The Gibbs adsorption equation is used to explain the origin of the inconsistency by linking the molecules adsorbed at the interface to the curvature corrections of the surface tension. The Tolman length and rigidity constant are determined for several water–alcohol mixtures and used to show that the corrected theory is free of physical inconsistencies and provides accurate predictions of the nucleation rates. In particular, for the ethanol-water and propanol-water mixtures, the average error in the predicted nucleation rates is reduced from 11–15 orders of magnitude to below 1.5. The curvature-corrected nucleation theory opens the door to reliable predictions of nucleation rates in multicomponent systems, which are crucial for applications ranging from atmospheric science to research on volcanos.

Most first order phase transitions, such as condensation, cavitation, boiling, and crystallization take place through a common mechanism known as nucleation. Here, the rate-limiting step is the formation of an incipient portion of the new phase exceeding the critical size required to continue growing spontaneously. This qualitative picture of the process is the basis of classical nucleation theory (CNT), which is the most popular model for predicting the rates of formation and properties of nucleating embryos [1–3]. For *pure* fluids, CNT is qualitatively correct [4–6]. However, the predicted rates show systematic deviations from experiments, with errors reaching 20 orders of magnitude for argon [7]. The discrepancies are hypothesized to stem from the crude approximations involved in CNT, especially the so-called capillary approximation, which considers the nucleus to be a spherical portion of a bulk phase with the same surface tension as the planar interface. Since the critical embryo is nanosized, much effort has been devoted to estimate curvature corrections for the surface tension and evaluate their impact on nucleation in pure fluids [8–15].

Most systems of interest are mixtures. Similar to pure fluids, CNT predictions for multicomponent nucleation rates can be off by many orders of magnitude. But more severely, even the qualitative picture of nucleation is in some cases wrong, as CNT can predict a *negative* number of particles in the critical embryo [16, 17]. Multicomponent CNT has therefore been rendered useless for many systems, such as binary mixtures of water and strongly interacting molecules like alkanols [16–19], or acetic acid [20]. Previous studies with density functional theory [21] and thermodynamics [22, 23] have suggested that the capillarity approximation might be the cause for this inconsistency, but a simple yet general remedy has been missing.

Using condensation of highly surface-active alcohol–water mixtures as example, we will show that incorporating curvature corrections for the surface tension in homogeneous nucleation theory removes the inconsistencies of multicomponent CNT. An explanation founded in thermodynamics will be provided on the basis of Gibbs adsorption equation. In addition to being physically consistent, the corrected theory yields quantitatively accurate predictions of nucleation rates, facilitating reliable predictions for applications ranging from atmospheric science [24] to research on volcanoes [25].

Condensation is an activated process that takes place through the formation of a critically-sized droplet in a supersaturated gas. In the context of CNT, the nucleation rate is given by

$$J = J_0 \exp\left(-\frac{W}{k_\mathrm{B}T}\right), \tag{1}$$

where W is the work of formation of the critical embryo, k_B is Boltzmann's constant and T is temperature. The kinetic prefactor, J_0, has in this work been calculated from the accurate expression by Vehkamäki and Ford [26], using a Zeldovich factor based on the virtual-monomer approach [2, 27].

The work of formation for the critical droplet is [1, 2]

$$W = \frac{4\pi}{3}\sigma R_\mathrm{t}^2\,, \tag{2}$$

This is the accepted version of an article published in Physical Review Letters
http://dx.doi.org/10.1103/PhysRevLett.124.045701

where R_t is the droplet's radius of tension and σ is the corresponding surface tension. We have chosen the radius of tension as dividing surface because it makes the final expressions particularly simple. To apply the theory in the general multicomponent case, one must specify how to calculate σ and R_t for a supersaturated gas with given pressure P^g and mole fractions $\boldsymbol{y}$. The critical droplet has an interior pressure P^ℓ, interior mole fractions $\boldsymbol{x}$, and surface tension $\sigma(R_\mathrm{t}, \boldsymbol{x})$. The curvature dependence of the surface tension is assumed to follow the Helfrich expansion [28, 29]:

$$\sigma(R_\mathrm{t}, \boldsymbol{x}) = \sigma_0(\boldsymbol{x})\left(1 - \frac{2\delta(\boldsymbol{x})}{R_\mathrm{t}}\right) + \frac{k_\mathrm{s}(\boldsymbol{x})}{R_\mathrm{t}^2}, \tag{3}$$

where $\sigma_0(\boldsymbol{x})$ is the planar surface tension. The Tolman length, $\delta(\boldsymbol{x})$, and spherical rigidity, $k_\mathrm{s}(\boldsymbol{x})$, referred to as the Helfrich coefficients, encode how the surface tension of droplets with interior composition $\boldsymbol{x}$ vary with curvature, $(1/R_\mathrm{t})$.

Similar to CNT, we assume ideal gas and incompressible liquid. This gives the following expressions for the chemical potentials of the gas (superscript g) and the liquid (superscript ℓ)

$$\mu_i^\mathrm{g}(\boldsymbol{y}, P^\mathrm{g}) = k_\mathrm{B}T \ln\left(\frac{P^\mathrm{g} y_i}{P_i^{\mathrm{sat,pure}}}\right), \tag{4}$$

$$\mu_i^\ell(\boldsymbol{x}, P^\ell) = k_\mathrm{B}T \ln a_i^\mathrm{sat}(\boldsymbol{x}) + \bar{v}_i(\boldsymbol{x})(P^\ell - P^\mathrm{sat}(\boldsymbol{x})). \tag{5}$$

Here $P_i^{\mathrm{sat,pure}}$ is the saturation pressure of pure component i, P^sat is the saturation pressure of the mixture, a_i^sat is its saturation activity, and $\bar{v}_i$ is its partial molecular volume; these are often tabulated [16]. The thermodynamic state at the interior of the critical droplet, given by $(P^\ell, \boldsymbol{x})$, is determined from equality of chemical potentials in the metastable gas and the interior of the droplet, i.e. Eq. (4) and Eq. (5).

Having obtained $(P^\ell, \boldsymbol{x})$ one next solves for R_t, which is given by the Laplace equation [1, 2]

$$P^\ell - P^\mathrm{g} = \frac{2\sigma(R_\mathrm{t}, \boldsymbol{x})}{R_\mathrm{t}}. \tag{6}$$

For CNT, Eq. (6) can be solved exactly:

$$R_\mathrm{CNT} = \frac{2\sigma_0}{P^\ell - P^\mathrm{g}}. \tag{7}$$

If $\sigma(R_\mathrm{t}, \boldsymbol{x})$ follows the Helfrich expansion however, the Laplace equation is a third-order polynomial in R_t. We solve this using a second-order perturbation expansion

$$R_\mathrm{t} \approx R_\mathrm{CNT}\left(1 + \frac{a}{R_\mathrm{CNT}} + \frac{b}{R_\mathrm{CNT}^2}\right), \tag{8}$$

where by inserting Eq. (8) into Eq. (6), we identify

$$a = -2\delta\,, \quad b = \frac{k_\mathrm{s}}{\sigma_0} - 4\delta^2. \tag{9}$$

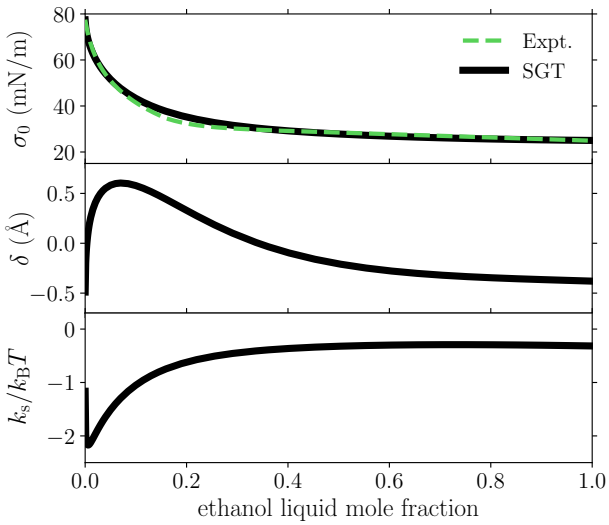

FIG. 1. Helfrich coefficients for the water–ethanol mixture at 260 K along the path of constant liquid composition. The experimental value of the surface tension is taken from Ref. 16.

With this approximation for R_t, Eq. (2) yields the work of formation beyond the capillarity approximation. The final equations are

$$R_\mathrm{t} \approx R_\mathrm{CNT}\left(1 - \frac{2\delta}{R_\mathrm{CNT}} + \frac{k_\mathrm{s}/\sigma_0 - 4\delta^2}{R_\mathrm{CNT}^2}\right), \tag{10}$$

$$W \approx \frac{4\pi\sigma_0 R_\mathrm{CNT}^2}{3}\left(1 - \frac{6\delta}{R_\mathrm{CNT}}\right) + 4\pi k_\mathrm{s}\,. \tag{11}$$

Eqs. (10)–(11) are the defining equations for the curvature-corrected CNT (c-CNT); they reduce to the standard expressions of CNT when $\delta = k_\mathrm{s} = 0$.

The next step in order to apply c-CNT is to determine the Helfrich coefficients. In Ref. [30], it was shown that square gradient theory (SGT) gave very similar Helfrich coefficients as full density functional theory with a basis in perturbed-chain polar statistical associating fluid theory, even for surface-active mixtures. Since the full density functional theory may give inaccurate predictions for alcohols [30], we have combined SGT with the cubic plus association (CPA) equation of state (EOS) to compute δ and k_s for several water–alcohol mixtures [31–33]. The methodology is detailed in [29, 30], and in the Supplementary Information (SI), which includes Refs. [34–41].

The Helfrich coefficients of the water–alcohol mixtures studied in this work exhibit a qualitatively similar behavior. They are displayed for the water–ethanol mixture in Fig. 1. The Tolman length and spherical rigidity both display a strong, nonlinear dependence on the ethanol mole fraction. Whereas δ and k_s are both negative for pure ethanol and water and thus partially cancel each other in Eq. (3), for the mixture they can have opposite signs and larger magnitudes. The Tolman length of pure water is $\sim$−0.5 Å, but becomes positive with only

This is the accepted version of an article published in Physical Review Letters
http://dx.doi.org/10.1103/PhysRevLett.124.045701

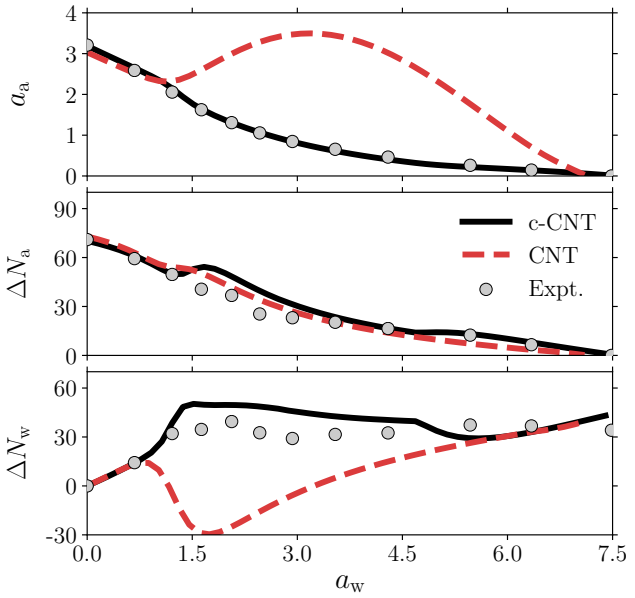

FIG. 2. Properties of critical droplets in the water–ethanol mixture at 260 K, corresponding to a nucleation rate $J^{\mathrm{spec}} = 10^{13}\,\mathrm{m^{-3}s^{-1}}$ for CNT and c-CNT, with experimental data from Ref. 16. Top: onset activities. Middle: excess ethanol content. Bottom: excess water content.

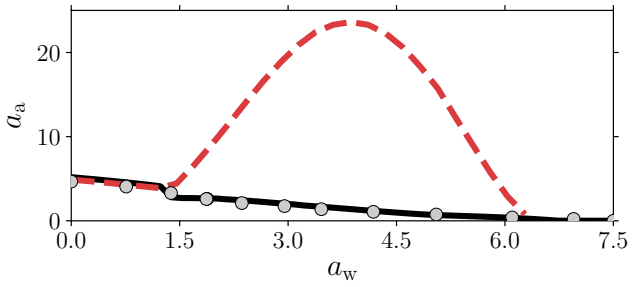

FIG. 3. Onset activities for water–propanol at 260 K, corresponding to a nucleation rate $J^{\mathrm{spec}} = 10^{13}\,\mathrm{m^{-3}s^{-1}}$ for CNT and c-CNT, with experimental data from Ref. 42.

0.35% ethanol mole fraction in the liquid phase; in the same range, the absolute value of the spherical rigidity nearly doubles. A minute concentration of the surface-active component can thus change the surface tension of a small cluster dramatically due to the strong surface adsorption. This observation is of high importance to atmospheric science, since surface-active components like sulfuric acid and ammonia can be present in low concentrations during formation of rain drops [24].

In multicomponent condensation, the degree of metastability is conveniently given in terms of gas activities, which for component i is defined as $a_i = P^{\mathrm{g}} y_i / P_i^{\mathrm{sat,pure}}$. For the water–alcohol mixtures at a given temperature, the nucleation rate $J(a_{\mathrm{a}}, a_{\mathrm{w}})$ is a function of the gas activities of the two components, where subscripts a and w denote alcohol and water, respectively. In binary nucleation experiments, it is customary to measure *onset activities*, defined as the values of the activities of the two components that yield a constant value of the nucleation rate $J(a_{\mathrm{a}}, a_{\mathrm{w}}) = J^{\mathrm{spec}}$, which for the experiments in Ref. 16 was set to $J^{\mathrm{spec}} = 10^{13}\,\mathrm{m^{-3}s^{-1}}$. Fig. 2-top displays the experimentally measured onset activities (circles), the infamous "hump" predicted by binary CNT [17] (dashed line), and the complete removal of this problem by c-CNT (solid line).

The hump represents an unphysical prediction of CNT. This can be explained by a closer inspection of the number of alcohol and water molecules in the critical droplet in excess over that of the metastable gas, ΔN_{a} and ΔN_{w}. Combining the first nucleation theorem [1, 2, 26],

$$\Delta N_i = k_{\mathrm{B}} T \left(\frac{\partial \ln J}{\partial \mu_i} \right)_{T,\mu_j}, \tag{12}$$

with Eq. (4) and the definition of a_i, one obtains [1, 2]

$$\left(\frac{\partial a_{\mathrm{a}}}{\partial a_{\mathrm{w}}} \right)_{J,T} = -\frac{a_{\mathrm{a}}}{a_{\mathrm{w}}} \frac{\Delta N_{\mathrm{w}}}{\Delta N_{\mathrm{a}}}. \tag{13}$$

Since $a_{\mathrm{a}}, a_{\mathrm{w}} > 0$, Eq. (13) implies that a positive slope in the onset-activity plot corresponds to a negative molecular content for one of the species. The second and third plots in Fig. 2 show the excess ethanol and water content of the droplets computed from Eq. (12), as well as the values inferred from the experiments of Ref. 16 using the first nucleation theorem [2, 43]. The plots should be interpreted with caution, as there are large uncertainties associated with the estimation of molecular content from binary nucleation experiments. In fact, the method used in Ref. 16 assumes that $\ln J$ is a linear function of $\sqrt{a_{\mathrm{a}}^2 + a_{\mathrm{w}}^2}$, which is a crude approximation even for pure components.

In any case, the most important point is that whereas CNT predicts a negative number of water molecules in the critical drop, c-CNT removes this inconsistency. More remarkably, for water–propanol (Fig. 3) and water–methanol (SI), c-CNT also completely removes the unphysical hump, although the phase behaviors of these mixtures at 260 K differ significantly from that of water–ethanol. In addition, for the onset activities of water–ethanol (Fig. 2-top) we verified that we obtain the same excellent agreement between experiments and c-CNT for nucleation rates that are 100 times higher or lower.

We shall next explain *why* the Helfrich expansion is successful in removing the inconsistencies of CNT. For a given metastable gas state, CNT and c-CNT predict the same interior mole fraction and interior pressure of the critical cluster. Fig. 4-top shows how the surface tension varies with curvature for CNT and c-CNT when the ethanol liquid mole fraction equals $x_{\mathrm{a}} = 0.1$. We have marked the point on each curve corresponding to the

This is the accepted version of an article published in Physical Review Letters
http://dx.doi.org/10.1103/PhysRevLett.124.045701

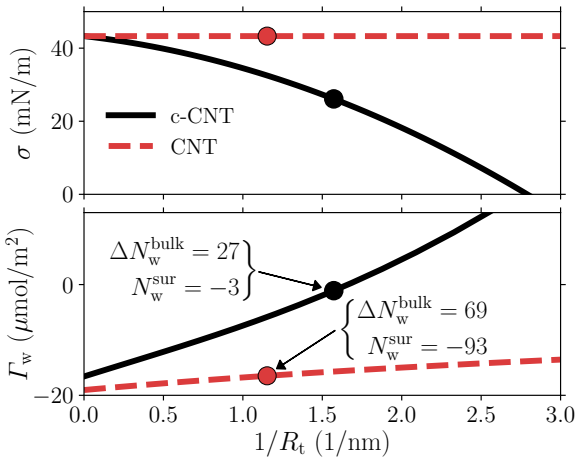

FIG. 4. Effect of Helfrich expansion on surface tension (top) and adsorption (bottom) for droplets of ethanol liquid mole fraction 0.1. The dashed line is the capillary approximation (CNT), and the marked critical droplet corresponds to a gas state yielding $J^{\mathrm{CNT}} = 10^{13}\,\mathrm{m^{-3}s^{-1}}$, having the indicated number of water particles in the interior ($\Delta N_{\mathrm{w}}^{\mathrm{int}}$) and the surface ($N_{\mathrm{w}}^{\mathrm{sur}}$). The full line is the Helfrich expansion (c-CNT), and the marked droplet corresponds to the *same gas state*.

gas state for which CNT predicts $J^{\mathrm{CNT}} = 10^{13}\,\mathrm{m^{-3}s^{-1}}$, which corresponds to a water activity of 2.1 in Fig. 2. By applying the Helfrich expansion, the surface tension is reduced from its planar value of 43 mN/m (CNT) to 26 mN/m in c-CNT, i.e. by 40%. A reduced surface tension means that lower gas activities are needed to yield a given nucleation rate. This explains why the Helfrich expansion lowers the onset activities with respect to the hump predicted by CNT in Fig. 2-top.

There is also a more direct way to see why curvature corrections fix the problem of negative water content. The excess number of water particles in the critical cluster can be split into contributions from the interior of the cluster ($\Delta N_{\mathrm{w}}^{\mathrm{int}}$) and the surface ($N_{\mathrm{w}}^{\mathrm{sur}}$) as

$$\Delta N_{\mathrm{w}} = \Delta N_{\mathrm{w}}^{\mathrm{int}} + N_{\mathrm{w}}^{\mathrm{sur}}, \tag{14}$$

where $\Delta N_{\mathrm{w}}^{\mathrm{int}} = \left(x_{\mathrm{w}}\rho^{\ell} - y_{\mathrm{w}}\rho^{\mathrm{g}}\right) 4\pi R_{\mathrm{t}}^3/3$ and ρ is the number density. The water adsorption is defined as $\Gamma_{\mathrm{w}} = N_{\mathrm{w}}^{\mathrm{sur}}/(4\pi R_{\mathrm{t}}^2)$. For all the cases considered in this work $\Delta N_{\mathrm{w}}^{\mathrm{int}}$ is positive, and the negative number of particles in the critical cluster originate in Γ_{w}. We computed the adsorption using Eq. (12) combined with Eqs. (5) and (14), and the result is plotted in Fig. 4-bottom. The effect of the Helfrich expansion on adsorptions is dramatic: whereas c-CNT predicts that only 3 water molecules are "missing" from the interface, CNT predicts 93; this discrepancy is primarily due to the adsorption Γ_{w} from CNT being a factor 15 larger in magnitude than for c-CNT.

The surface tension and the adsorptions are linked by Gibbs adsorption equation [29, 44]

$$\mathrm{d}\sigma = -\boldsymbol{\Gamma}\cdot\mathrm{d}\boldsymbol{\mu}\,, \tag{15}$$

TABLE I. Statistics for the logarithmic deviations $\log_{10}(J/J^{\mathrm{expt}})$ from the experimental rates J^{expt} of Refs. 16 and 42. The average and median are calculated using absolute values of the logarithmic deviations.

Method	min	max	average	median
ethanol–water				
CNT	−21.3	−0.2	10.9	12.7
c-CNT	−2.3	0.9	0.8	0.5
1-propanol–water				
CNT	−35.2	1.5	14.8	9.5
c-CNT	−2.7	2.9	1.5	1.2

where $\boldsymbol{\Gamma}$ is the vector of adsorptions. By differentiating Eq. (15) with respect to R_{t}, approximating $\Delta P \approx P^{\ell}$, using Eq. (5) and rearranging we find

$$\bar{v}_{\mathrm{a}}\Gamma_{\mathrm{a}} + \bar{v}_{\mathrm{w}}\Gamma_{\mathrm{w}} = \underbrace{-\left(\frac{\partial\sigma}{\partial R_{\mathrm{t}}}\right)_{T,x_{\mathrm{w}}} \Big/ \left(\frac{\partial P^{\ell}}{\partial R_{\mathrm{t}}}\right)_{T,x_{\mathrm{w}}}}_{\Delta\Gamma}. \tag{16}$$

Since $\bar{v}_{\mathrm{a}}/\bar{v}_{\mathrm{w}} \approx 4$, the adsorptions of water and ethanol in CNT are always with opposite sign, with the water adsorption being nearly four times larger in magnitude. Using the derivatives of Eqs. (3) and (6) in Eq. (16) gives

$$\Delta\Gamma = 0, \qquad \text{for CNT,} \tag{17}$$

$$\Delta\Gamma \approx \delta + (4\delta^2 - k_{\mathrm{s}}/\sigma_0)/R_{\mathrm{t}} \qquad \text{for c-CNT.} \tag{18}$$

Eq. (17) is a well-known result [2, 22]. Eq. (18), however, is new, and accounts for most of the difference between the two curves in Fig. 4-bottom. It constitutes a salient demonstration of why the curvature-dependence of the surface tension is crucial to capturing the adsorptions. This is especially important for surface-active mixtures, where Tolman lengths and spherical rigidities can far exceed their pure-component values (cf. Fig. 1).

Besides removing the inconsistencies of CNT, curvature corrections also yield accurate predictions for binary nucleation rates. For ethanol–water and propanol–water, the nucleation rates predicted from c-CNT display a remarkable agreement with experimental results, in contrast to those from CNT (see Tab. I and the SI). In addition to bringing the average order-of-magnitude deviation below 1.5, c-CNT has worst-case deviations below three orders of magnitude—in sharp contrast to CNT, which can underpredict the nucleation rates by 35 orders of magnitude for water–propanol. To evaluate the impact of the assumption of ideal gas and incompressible liquid on the nucleation rate predictions, we replaced Eqs. (4)–(5), evaluated with the correlations of Ref. 16, with the chemical potentials from the CPA EoS. This changed the numbers in Tab. I by less than 1.5. Non-idealities are thus not essential at these conditions. Furthermore, the conclusions drawn in this work are not sensitive to the

This is the accepted version of an article published in Physical Review Letters
http://dx.doi.org/10.1103/PhysRevLett.124.045701

EOS used in SGT, as we also tested that another EOS (PC-SAFT [45, 46], not shown) yields similar results.

In conclusion, we have demonstrated that adding a second-order curvature expansion of the surface tension corrects the composition-dependence of the work of formation in binary CNT, removes the unphysical predictions of negative molecular content in the critical nucleus, and yields simple yet accurate predictions of nucleation rates. The approach involves no fitting to nucleation measurements; only planar surface tensions and an accurate equation of state are needed to calculate the Tolman length and rigidity parameters. c-CNT may be the key to quantitative predictions of condensation and cavitation rates for mixtures relevant to industrial processes, atmospheric science, and climate-change modeling.

We thank Titus Sebastian van Erp, Hans Langva Skarsvåg and Phillipp Rehner for helpful input. This work has been partially funded by the Spanish *Ministerio de Economía y Competitividad* through Grants FIS2015-67837-P and PGC2018-098373-B-I00. The authors were supported by the Norwegian Center of Excellence *PoreLab*.

* ailo.aasen@ntnu.no

[1] D. Kashchiev, *Nucleation: Basic Theory with Applications* (Butterworth–Heinemann, Oxford, 2000)
[2] H. Vehkamäki, *Classical Nucleation Theory in Multicomponent Systems* (Springer Verlag, Berlin, 2006)
[3] V. Kalikmanov, *Nucleation Theory* (Springer Verlag, Berlin, 2013)
[4] Y. Viisanen, R. Strey, and H. Reiss, J. Chem. Phys. **99**, 4680 (1993)
[5] J. Wedekind, D. Reguera, and R. Strey, J. Chem. Phys. **127**, 064501 (2007)
[6] R. McGraw and A. Laaksonen, Phys. Rev. Lett. **76**, 2754 (1996)
[7] K. Iland, J. Wölk, R. Strey, and D. Kashchiev, J. Chem. Phys. **127**, 154506 (2007)
[8] R. McGraw and A. Laaksonen, J. Chem. Phys. **106**, 5284 (1997)
[9] J. C. Barrett, J. Chem. Phys. **124**, 144705 (2006)
[10] A. E. van Giessen and E. M. Blokhuis, J. Chem. Phys. **131**, 164705 (2009)
[11] E. M. Blokhuis and A. E. van Giessen, J. Phys.: Condens. Matter **25**, 225003 (2013)
[12] Ø. Wilhelmsen, D. Bedeaux, and D. Reguera, J. Chem. Phys. **142**, 171103 (2015)
[13] N. Bruot and F. Caupin, Phys. Rev. Lett. **116**, 056102 (2016)
[14] S. Kim, D. Kim, J. Kim, S. An, and W. Jhe, Phys. Rev. X **8**, 041046 (2018)
[15] V. D. Nguyen, F. C. Schoemaker, E. M. Blokhuis, and P. Schall, Phys. Rev. Lett. **121**, 246102 (2018)
[16] Y. Viisanen, R. Strey, A. Laaksonen, and M. Kulmala, J. Chem. Phys. **100**, 6062 (1994)
[17] M. Kulmala, A. Lauri, H. Vehkamäki, A. Laaksonen, D. Petersen, and P. Wagner, J. Phys. Chem. B **105**, 11800 (2001)
[18] K. Neumann and W. Döring, Z. Phys. Chem. **186**, 203 (1940)
[19] S. Tanimura, H. Pathak, and B. E. Wyslouzil, J. Chem. Phys. **139**, 174311 (2013)
[20] W. Studziński, G. Spiegel, and R. Zahoransky, J. Chem. Phys. **84**, 4008 (1986)
[21] A. Laaksonen and I. Napari, J. Phys. Chem. B **105**, 11678 (2001)
[22] A. Laaksonen, R. McGraw, and H. Vehkamäki, J. Chem. Phys. **111**, 2019 (1999)
[23] Y. S. Djikaev, I. Napari, and A. Laaksonen, J. Chem. Phys. **120**, 9752 (2004)
[24] M. Kulmala, H. Vehkamäki, T. Petäjä, M. Dal Maso, A. Lauri, V. M. Kerminen, W. Birmili, and P. H. McMurry, J. Aerosol Sci. **35**, 143 (2004)
[25] D. R. Baker, F. Brun, C. O'Shaughnessy, L. Mancini, J. L. Fife, and M. Rivers, Nat. Commun. **3**, 1135 (2012)
[26] H. Vehkamäki and I. J. Ford, J. Chem. Phys. **113**, 3261 (2000)
[27] M. Kulmala and Y. Viisanen, J. Aerosol Sci. **22**, S97 (1991)
[28] W. Helfrich, Z. Naturforsch. C **28**, 693 (1973)
[29] A. Aasen, E. M. Blokhuis, and Ø. Wilhelmsen, J. Chem. Phys. **148**, 204702 (2018)
[30] P. Rehner, A. Aasen, and Ø. Wilhelmsen, J. Chem. Phys. **151**, 244710 (2019)
[31] G. M. Kontogeorgis, E. C. Voutsas, I. V. Yakoumis, and D. P. Tassios, Ind. Eng. Chem. Res. **35**, 4310 (1996)
[32] A. J. Queimada, C. Miqueu, I. M. Marrucho, G. M. Kontogeorgis, and J. A. P. Coutinho, Fluid Phase Equilib. **228**, 479 (2005)
[33] M. Oliveira, I. Marrucho, J. Coutinho, and A. Queimada, Fluid Phase Equilib. **267**, 83 (2008)
[34] M. Hongo and T. Hibino, Kagaku Kogaku Ronbunshu **15**, 863 (1989)
[35] G. Soave, Chem. Eng. Sci. **27**, 1197 (1972)
[36] P. Cornelisse, *The Gradient Theory Applied - Simultaneous Modelling of Interfacial Tension and Phase Behaviour*, Ph.D. thesis, Delft University of Technology (1997)
[37] A. Aasen, M. Hammer, G. Skaugen, J. Jakobsen, and Ø. Wilhelmsen, Fluid Phase Equilib. **442**, 125 (2017)
[38] A. Mulero, I. Cachadiña, and E. L. Sanjuán, J. Phys. Chem. Ref. Data **44**, 033104 (2015)
[39] T. Petrova and R. B. Dooley, *Revised release on surface tension of ordinary water substance*, Tech. Rep. (IAPWS, 2014) `http://www.iapws.org`
[40] G. Vasquez, E. Alvarez, and J. M. Navaza, J. Chem. Eng. Data **40**, 611 (1995)
[41] S. Tanimura, U. M. Dieregsweiler, and B. E. Wyslouzil, J. Chem. Phys. **133**, 174305 (2010)
[42] R. Strey, Y. Viisanen, and P. Wagner, J. Chem. Phys. **103**, 4333 (1995)
[43] D. Kashchiev, J. Chem. Phys. **76**, 5098 (1982)
[44] J. Gibbs, *The Scientific Papers of J. Willard Gibbs* (Ox Bow Press, London, 1993)
[45] J. Gross and G. Sadowski, Ind. Eng. Chem. Res. **40**, 1244 (2001)
[46] J. Gross and G. Sadowski, Ind. Eng. Chem. Res. **41**, 5510 (2002)

This is the accepted version of an article published in Physical Review Letters
http://dx.doi.org/10.1103/PhysRevLett.124.045701